Robust correlations between action potential duration and the properties of synaptic connections in layer 4 interneurones in neocortical slices from juvenile rats and adult rat and cat

Afia B. Ali, A. Peter Bannister and Alex M. Thomson

Department of Pharmacology, The School of Pharmacy, London University, 29–39 Brunswick Square, London WC1N 1AX, UK

Many studies of cortical interneurones use immature rodent tissue, while many recordings *in vivo* are made in adult cats. To determine the extent to which interneuronal circuitry studied with one approach can transfer to another, we compared layer 4 interneurones and their local connections across two age groups and two species and with similar connections in layers 3 and 5, using two common recording techniques: dual whole cell recordings at 20°C and dual sharp electrode recordings at 35°C. In each group, a range of morphological and electrophysiological characteristics was observed. In all groups, however, positive correlations were found between the width of the action potential and rise times and widths at half-amplitude of EPSPs and IPSPs and the EPSP paired pulse ratio. Multipolar interneurones with narrow spikes generated the fastest IPSPs in pyramidal cells and received the briefest, most strongly depressing EPSPs, while bitufted interneurones with broader spikes and adapting and burst firing patterns activated the broadest IPSPs and received the slowest, most strongly facilitating/augmenting EPSPs. Correlations were similar in all groups, with no significant differences between adult rat and cat, or between layers, but events were four times slower in juveniles at 20°C. Comparisons with previous studies indicate that this is due in part to age, but in large part to temperature. Studies in adults were extended with detailed analysis of synaptic dynamics, which appeared to decay more rapidly than at juvenile connections. EPSPs exhibited the complexity in time course of facilitation, augmentation and depression previously described in other adult neocortical connections. That is, the time course of recovery from facilitation or depression rarely followed a simple smooth exponential decay. Facilitation and depression were not always maximal at the shortest interspike intervals, and recovery was often interrupted by peaks and troughs in mean EPSP amplitude with a periodicity around 80 Hz.

(Received 3 November 2006; accepted after revision 12 January 2007; first published online 18 January 2007)
Corresponding author A. M. Thomson, Department of Pharmacology, The School of Pharmacy, London University, 29–39 Brunswick Square, London WC1N 1AX, UK. Email: alex.thomson@pharmacy.ac.uk

Neocortical interneurones display many morphological (e.g. Ramón y Cajal, 1911; Lund, 1973, 1987; Jones, 1975; Houser *et al.* 1984; Lund & Lewis, 1993) and physiological characteristics (e.g. Kawaguchi & Kubota, 1993, 1996, 1997, 1998; Kubota & Kawaguchi, 1997; Cauli *et al.* 1997; Gupta *et al.* 2000; Wang *et al.* 2002, 2004; Beierlein *et al.* 2003). There remains much debate about how many classes of neocortical interneurones there are and whether all can be classified into distinct subclasses. In the single layered hippocampal CA1 region, at least 16 classes can be identified by the position and shape of dendritic and axonal arbors, cellular marker expression and postsynaptic target preference (Somogyi & Klausberger, 2005). Moreover, the functional diversity of these several types is indicated by distinct patterns of activity during pronounced theta rhythm and sharp waves (Klausberger *et al.* 2003, 2004, 2005). Some classes of neocortical interneurones with distinctive morphologies can be similarly identified: chandelier or axo-axonic cells targeting pyramidal axon initial segments (Somogyi, 1977) and dendrite-preferring Martinotti (Martinotti, 1889), double bouquet and neurogliaform cells (Ramón y Cajal, 1911).

Interneurones targeting somata and proximal pyramidal dendrites, i.e. basket cells, are typically multipolar, often immunopositive for parvalbumin and display fast spiking behaviour (e.g. Cauli *et al.*

 DOI: 10.1113/jphysiol.2006.124214

1997; Kawaguchi & Kubota, 1997). In contrast, dendrite-preferring cells, including Martinotti (Wang *et al.* 2004) and double bouquet cells (Buhl *et al.* 1997; Tamas *et al.* 1997), have more vertically orientated bitufted dendrites, more commonly display adapting/burst firing behaviour and are immunopositive for, for example, somatostatin.

There are, however, many interneurones that cannot be readily classified. Extending the analogy with hippocampus, CA1 has at least eight classes targeting pyramidal dendrites, five innervating intermediate dendrites also innervated by Schaffer collaterals and three innervating distal apical dendrites (Somogyi & Klausberger, 2005). Moreover, the six-layered neocortex provides a richer target choice. Some interneurones ramify solely within their layer of origin, some innervate two adjacent layers, others two non-adjacent layers (Lund, 1988; Thomson *et al.* 1996), while many dendrite-preferring interneurones innervate several adjacent layers without apparent preference. Moreover, in neocortex, the target layer cannot identify the cells or subcellular compartments innervated, since all layers contain somata, distal and proximal dendrites and axon initial segments.

Another complication is provided by the range of ages and species studied, the recording conditions and the uncertainty, therefore, as to whether findings in one species, at one age, studied with one technique, can form a basis from which conclusions associated with another can be drawn. We therefore compared layer 4 interneurones in two age groups and two species using different recording techniques; dual whole cell recordings of postnatal day 18–22 rat interneurones at 20°C and dual sharp electrode recordings of adult rat and cat interneurones at 35°C. We first addressed an essentially simple question, namely, are there fundamental properties of interneurones that correlate with the properties of their synaptic connections? Studies of adult EPSPs were extended to determine whether the more complex time courses of recovery from depression and facilitation apparent at other connections (West *et al.* 2006) are also expressed at excitatory connections onto layer 4 interneurones.

Methods

Dual intracellular recordings using sharp microelectrodes were made from synaptically connected neurones in slices of young adult rat somatosensory and visual cortex and in cat visual cortex as previously described (Thomson & West, 2003). Dual whole cell recordings were made from synaptically connected pairs of neurones in slices from postnatal day 18–22 rat somatosensory cortex as previously described (Ali & Nelson, 2006).

Slice preparation

Male Sprague–Dawley rats, 120–230 g body weight ($n = 50$), were anaesthetized with inhaled halothane (Fluothane) and intraperitoneal pentobarbitone sodium (Sagatal, or Euthetal; Rhone Merieux, Harlow, UK; > 60 mg kg^{-1}). Juvenile (postnatal day 18–22, $n = 89$) rats were anaesthetized with Euthetal. Male cats ($n = 7$, 2.5–3.4 kg) were anaesthetized intravenously with a mixture of α-chloralose (70 mg kg^{-1}) and pentobarbitone sodium (6 mg kg^{-1}) for a different series of experiments (procedures similar to Wang & Ramage, 2001), and each cat provided slices for three parallel experiments. Rats were perfused transcardially and cats (following an overdose of barbiturate) via the carotid arteries, with ice-cold modified artificial cerebrospinal fluid (ACSF) with added pentobarbitone (60 mg l^{-1}) in which 248 mM sucrose replaced NaCl. Rats were decapitated and the brain removed. Visual cortex was removed from cats via a hole in the skull. All procedures complied with UK Home Office regulations for animal use.

Coronal slices of adult neocortex, 450–500 μm thick (Vibroslice, Camden Instruments, Loughborough, UK) were cut and transferred to an interface recording chamber. Slices were maintained for 1 h in sucrose-containing medium, before switching to standard ACSF containing (mM): 124 NaCl, 25.5 $NaHCO_3$, 3.3 KCl, 1.2 KH_2PO_4, 1.0 $MgSO_4$, 2.5 $CaCl_2$ and 15 D-glucose, equilibrated with 95% O_2–5% CO_2 at 35–36°C.

Coronal slices of juvenile neocortex 300–330 μm thick were incubated for at least 1 h in ACSF containing (mM): 121 NaCl, 2.5 KCl, 1.25 NaH_2PO_4, 2 $CaCl_2$, 1 $MgCl_2$, 26 $NaHCO_3$, 20 glucose and 5 pyruvate, equilibrated with 95% O_2–5% CO_2. For recordings, slices were transferred to a submerged-style chamber and perfused with ACSF at 1–2 ml min^{-1} at 20–24°C.

Dual recordings

In adult rat and cat slices, paired intracellular recordings were made with conventional sharp microelectrodes, containing 2 M $KMeSO_4$ and 2% w/v biocytin (tip resistance 90–150 MΩ). Presynaptic neurones were depolarized with combinations of square-wave and ramped currents, typically delivered at one pulse per 3 s to elicit trains of action potentials (APs) at different frequencies, and postsynaptic responses were recorded (filtered at 5 kHz, digitized at 10 kHz; Spike2, Cambridge Electronic Design, Cambridge, UK). The time course of recovery from synaptic depression or facilitation may not be adequately described by a simple exponential function. Nor can it be fully explored using a finite number of well-spaced interspike intervals that are identical, in any one trial, for all spikes in the train (Thomson & West, 2003; West *et al.* 2006; A. P. Bannister & A. Thomson,

unpublished observations). The size and shape of the current pulse was therefore altered continuously to elicit a range of interspike intervals and firing patterns.

In juvenile slices, dual whole cell recordings were made in layers 3, 4 and 5. Interneurones with round or bitufted somata were selected using videomicroscopy under near-infrared differential interference contrast (DIC) illumination and recorded simultaneously with pyramidal cells. Patch pipettes (resistance 8–10 MΩ) were pulled from borosilicate glass tubing and filled with an internal solution containing (mM): 144 potassium gluconate, 3 $MgCl_2$, 0.2 EGTA, 10 Hepes, 2 Na_2-ATP, 0.2 Na_2-GTP and 0.02% w/v biocytin (pH 7.2–7.4, 300 mosmol l^{-1}). Presynaptic neurones were depolarized above firing threshold with brief 5–10 ms square-wave currents, typically delivered at one pulse, one pair of pulses or one brief train of pulses (20 or 67 Hz) per 2 s. Postsynaptic responses were recorded for off-line analysis (filtered at 2 kHz, digitized at 5 kHz; Signal software, Cambridge, UK). In both adults and juveniles, AP width at half-amplitude (AP HW) was measured from APs elicited by just suprathreshold depolarizing square-wave current pulses, the AP amplitude being measured from the start of the fast rising phase to the peak. Membrane time constants were measured from the voltage responses to small current pulses (0.2–0.4 nA) delivered from membrane potentials between −65 and −70 mV.

Biocytin labelling and histological processing

Cells were filled with biocytin and slices fixed, washed and resectioned at 50 μm. Interneurones filled using sharp electrodes were tested with a double immunofluorescence protocol that included fluorescently labelled avidin to identify cellular markers such as parvalbumin in recorded cells. Slices were then processed histologically [avidin–HRP/diamino benzidine (DAB)] for identification of recorded neurones as previously described (Hughes *et al.* 2000). Connected cell pairs were drawn in their entirety at ×1000 magnification using a drawing tube.

Off-line data analysis

Using in-house software, data sets in which the first EPSP/IPSP shape and amplitude and the postsynaptic membrane potential were stable, were selected. Single sweeps were checked individually to ensure that every presynaptic AP was recognized by the software and that the trigger points used for subsequent analysis were accurately aligned with the fast component of the rising phase of each AP. Sweeps that included artifacts or large spontaneous events were excluded from averaged records. Sweeps in which the second AP followed the first within a given time window were then selected and the second EPSP/IPSP within each of these windows averaged, using the rising phase of the second AP as the trigger. This second EPSP/IPSP average was superimposed on an average of all responses to single APs. The amplitude of the averaged second EPSP/IPSP was then measured from its peak to the appropriate point on the falling phase of the averaged first EPSP/IPSP. Averaged responses to later APs in trains were analysed similarly. In Figs 2–7, all illustrated EPSPs/IPSPs are averages or composite averages, each component including between 20 and 200 sweeps.

Where EPSPs exhibited an adequate signal-to-noise ratio, single sweep events were also measured, with cursors. To measure short interval second and subsequent EPSP amplitudes, an average of all single spike EPSPs was scaled to match the amplitude of the first EPSP in each sweep and the second EPSP amplitude measured from its peak to the appropriate point on the decay of the scaled first EPSP average. From larger adult data sets, single sweep EPSP amplitudes were plotted against interspike interval and smoothed (running average of 10–20 points) to reveal trends. To compare the contributions made by the first EPSP amplitude and the interspike interval, respectively, towards determining the second EPSP amplitude, the second EPSP amplitude was plotted against these two parameters. The combined effects of the interval between the first and second AP (first interspike interval) and the interval between the second and thirdrd AP (second interspike interval) on the amplitude of the third EPSP was tested by plotting the third EPSP amplitude against these two interspike intervals. The resulting three-dimensional surface plots were then rendered as contour maps with second or third EPSP amplitudes indicated by colour (PSI-Plot, Poly Software, International Inc., New York, NY, USA; Figs 5–7).

In Figs 5–7, averaged EPSPs elicited by second and subsequent spikes in trains are colour-coded according to their amplitude (blue indicates a small and red a large average amplitude). In composite averaged traces comprising averaged responses to each of several spikes in trains, fine lines represent the extrapolated decay of each EPSP derived from the decay of a similar amplitude EPSP. Capacitance coupling artifacts associated with the presynaptic spike recorded with sharp electrodes were removed graphically.

Statistical analysis

To determine whether correlations between interneuronal electrophysiological properties and the properties of their synaptic connections existed and whether these were similar across species and age groups, action potential (AP) width at half-amplitude, the amplitude and width at half-amplitude of the AP after-hyperpolarization (AP-AHP), EPSP/IPSP 10–90% rise time and width at half-amplitude were measured. Action potential amplitude was measured from the start of its fast rising

phase to its peak, and AP-AHP amplitude from the start of the fast rising phase of the AP to the peak of the AP-AHP. These parameters were plotted against each other and tested for correlations (PSI-Plot). Whether the distributions of these parameters differed across species and age groups was tested using Student's unpaired *t* test.

Statistical analysis was performed to determine whether the 'peaks and troughs' apparent in plots of EPSP amplitude against interspike interval (see Figs 5–7) resulted from populations of EPSPs with significantly different mean amplitudes. Subsets of single sweep EPSP amplitude measurements within narrow preceding interspike interval ranges (2–5 ms wide) were selected. This resulted in between five and 10 subsets of second or third EPSP amplitudes for each connection corresponding to peaks and troughs in the plots. To test the significance of the peaks and troughs apparent in the three-dimensional contour plots of third EPSP amplitude, subsets of single sweep third EPSP amplitude measurements were selected, each associated with narrow ranges of the two preceding interspike intervals. The means of these data subsets were compared using analysis of variance (one-way ANOVA) after testing for homogeneity of variance and multiple pairwise unpaired *t* tests subjected to the Bonferroni correction.

Results

This study includes recordings from 43 adult cat layer 4 interneurones, 28 adult rat layer 4 and 12 layer 3 interneurones, and 40 juvenile rat layer 3–5 interneurones, each tested with between one and six simultaneously recorded excitatory cells (pyramidal, or spiny stellate cells). A total of 125 such pairs tested in cats, 70 in adult rats and 89 in juvenile rats yielded the excitatory and inhibitory connections reported here. The more detailed descriptions result from 26 layer 4 pairs in adult cat visual cortex from which stable EPSPs and/or IPSPs were recorded, and nine layer 4 and eight layer 3 pairs involving interneurones in adult rat neocortical slices. The juvenile connections reported here involved eight interneurones in layer 4 of somatosensory cortex, 11 in layer 5 and 14 in layer 3 of somatomotor cortex. All illustrated interneurones were in layer 4. Some of the measurements included in population data were taken from cells for which other parameters have been published, but all of the illustrated pairs and the analysis presented here are new.

Firing properties of interneurones

The firing properties of these interneurones included cells with narrow spikes that showed little or no spike accommodation or frequency adaptation (5 in cats, Supplementary Fig. 1; and 18 in juvenile rats, Fig. 2*Ab*) and cells with narrow spikes that stopped firing abruptly and/or 'stuttered' during a suprathreshold depolarization (6 in adult rats and 12 in adult cats, Fig. 6*A*). These APs had widths at half-amplitude of 0.2–0.3 and 0.8–1.3 ms in adults and juveniles, respectively, and deep AP-AHPs (13–28 mV in adults and 8–20 mV in juveniles). With larger depolarizing pulses, or ramp currents, all such adult cells could maintain firing at frequencies above 350 Hz with little spike accommodation or frequency adaptation (e.g. the stopping/stuttering cells in Fig. 4 and Supplementary Figs 3 and 4). Cells with adapting firing patterns, i.e. where firing continued throughout a suprathreshold square-wave depolarizing pulse, but with a steadily decreasing rate of firing (Fig. 2*Ba*), exhibited APs with a wide range of widths at half-amplitude (0.2–0.6 ms in adults and 1.2–1.8 ms in juveniles) and a correspondingly wide range of AP-AHP amplitudes (Fig. 1*E*). Six interneurones in adult rats and three in cats with broad APs (0.4–0.6 ms) displayed burst firing characteristics and pronounced spike accommodation (Supplementary Fig. 2). Interneurones with burst firing patterns were not recorded in juveniles in this study. Finally, five interneurones with broad APs displayed a stuttering/stopping pattern (e.g. the bipolar interneurone in Supplementary Fig. 5) very similar to that displayed by some cells with narrow spikes except for the broader spike width and lower firing rates.

Correlations between interneuronal firing properties and morphology

In juvenile rats, all cells ($n = 19$) that had narrow APs (width at half-amplitude ≤ 1.3 ms), whether they were continuous spiking or adapting, were multipolar cells (Fig. 2) whose somata appeared round under infrared differential interference contrast microscopy (IR-DIC). In the majority, the axonal arbor was confined to the layer of origin and the proximal portion of one adjacent layer. Membrane time constants were 20.6 ± 2.5 ms in multipolar cells with narrow spikes. The cells with broader APs (width at half-amplitude 1.3–2.3 ms) typically displayed longer membrane time constants 28.4 ± 7.4 ms ($n = 12$) and were bitufted interneurones (Fig. 3), five with an axon that ramified densely superficial to the soma and extended to layer 1, and therefore classifiable as Martinotti cells.

A similar pattern was apparent in the adult. The large, multipolar, parvalbumin-immunopositive layer 4 interneurones in both species (Figs 4 and 6 and Supplementary Figs 1 and 3) often had partly myelinated axons and displayed narrow APs (width at half-amplitude ≤ 0.3 ms) with continuous or stopping/stuttering or adapting behaviour, input resistances of 41.6 ± 9.0 MΩ, and brief membrane time constants (5.27 ± 2.75 ms, $n = 15$). As can be seen from the figures, these cells had very disparate axonal arbors, with approximately equal

proportions of cells whose axons were confined to the layer of origin (e.g. Supplementary Fig. 1), those whose axons arborized most densely in two non-adjacent layers, typically layers 4 and 6 (e.g. Fig. 4), those that arborized almost equally in two or more adjacent layers (e.g. Fig. 6) and those that arborized extensively in layer 4 and sent a narrow focused axonal arbor to the deep layers (see Supplementary Fig. 3).

Cells displaying the broadest APs (width at half-amplitude 0.4–0.6 ms) typically displayed a higher input resistance (51.8 ± 11.3 MΩ), longer membrane time constants (9.4 ± 2.0 ms, $n = 8$) and stopping, adapting or burst firing characteristics. These cells were either bitufted or bipolar interneurones (Supplementary Fig. 5) and included two Martinotti-like cells (Fig. 7) and one double bouquet cell in a cat (Supplementary Fig. 2). These axons were rarely myelinated. Adult interneurones with intermediate spike widths included four large multipolar interneurones with complex or rounded AP-AHPs and a neurogliaform cell, all with adapting firing patterns, and two bipolar dendrite-preferring cells with non-adapting firing patterns.

The axonal arbors of interneurones were not significantly different in overall dimensions across the three populations. For example, multipolar cells with fast spikes that were confined to layer 4 were 492 ± 387 μm wide and 421 ± 216 μm tall in cats ($n = 5$), 360 ± 186 μm wide and 485 ± 48 μm tall in adult rats ($n = 3$) and 404 ± 58 μm wide and 430 ± 95 μm tall in juvenile rats ($n = 4$). The widest layer 4 axonal arbor from a multipolar cell filled and recovered in a cat slice was wider than the widest found in a rat (1174 cf. 704 μm), but amongst multipolar layer 4 interneurones that sent axons to the deeper layers, rat layer 4 cells were not dramatically different in vertical extent from cat layer 4 cells (up to 1182 μm in rats cf. 1321 μm in cats). Nor were layer 4 Martinotti cells larger in cats (477 ± 121 μm wide and 634 ± 65 μm tall, $n = 3$) than in juvenile rats (403 ± 135 μm wide and 631 ± 152 μm tall, $n = 3$). This, perhaps surprising, finding may reflect the wide diversity of interneurones presented in this study, but parallels a recent study of layer 4 pyramidal cells in which adult rat and cat cells with similar properties were not found to differ significantly in size (Bannister & Thomson, 2006).

Thus the prime difference between adult and juvenile interneurones was in the briefer time course of events such as APs and membrane time constants in adult tissue.

Connectivity ratios

In juvenile slices in which the interneurone and pyramidal cell and their relative positions were selected under IR-DIC, the probability of tested pairs being synaptically connected was very high and similar to those reported previously (Beierlein *et al.* 2003). Every pair tested ($n = 11$) that included a multipolar cell with a narrow AP yielded an EPSP and one in three (23/69) yielded an IPSP. Three of these connections were reciprocal (e.g. Fig. 2). In these pairs, the two neurones were extremely close neighbours, with their somata within a few microns of each other. In the 33 pairs tested in which the interneurone was a bitufted cell, one in four pairs yielded an EPSP and one in three an IPSP. Four connections were reciprocal (e.g. Fig. 3). For these pairs, pyramidal partners directly above or below the interneurone and within 50 μm of its soma were selected for testing.

In adult slices, 'blind' sharp electrode recordings were used and tested pairs were typically further apart, between 20 and 200 μm. In cat layer 4 pairs in which one cell was a continuous spiking interneurone with a narrow AP and the other a pyramid, one in 14 yielded an EPSP and one in 6.4 an IPSP. In pairs in which the interneurone had an intermediate AP duration and an adapting or stopping firing pattern, one in 16 yielded an EPSP and one in three an IPSP. Finally, in tests involving broad AP interneurones with adapting or burst firing behaviour, one in two yielded an EPSP and one in five an IPSP. These yielded an overall average 'hit rate' for EPSPs in cat layer 4 interneurones of one in 10, and for IPSPs of one in five. In adult rat layer 4 the average 'hit rate' for all types of layer 4 interneurones tested was one in seven for EPSPs and one in nine for IPSPs. Pooling data from layer 3 and layer 4, the average hit rate for rat interneurones with narrow spikes (half-width < 0.3 ms) was one in 10 for EPSPs and one in nine for IPSPs. For interneurones with broader APs (half-width > 0.3 ms) the rates were one in four for EPSPs and one in seven for IPSPs.

Since the paired recording tests performed in juvenile tissue were in most cases between more closely neighbouring cells than the tests in adult tissue, a direct comparison of 'hit rates' is slightly ambiguous. However, the higher rates observed in juvenile slices may also reflect a phase of high connectivity that precedes late developmental pruning.

Correlations between interneuronal properties and synaptic potential properties

The properties of the EPSPs and IPSPs reported here are summarized in Table 1. The amplitudes of EPSPs and IPSPs in juveniles were, on average, smaller than in adults ($P < 0.03$). Previous studies in adult rat slices had suggested that layer 5 interneurones with narrow spikes generate briefer IPSPs in pyramidal cells than interneurones with broad APs (Thomson *et al.* 1996), while in juvenile rats, fast spiking cells were reported to receive briefer EPSPs than low threshold spiking cells, but the time course of IPSPs generated by these two groups was reported to be similar (Beierlein *et al.* 2003). To determine whether relationships between interneuronal AP width at half-amplitude and synaptic properties exist

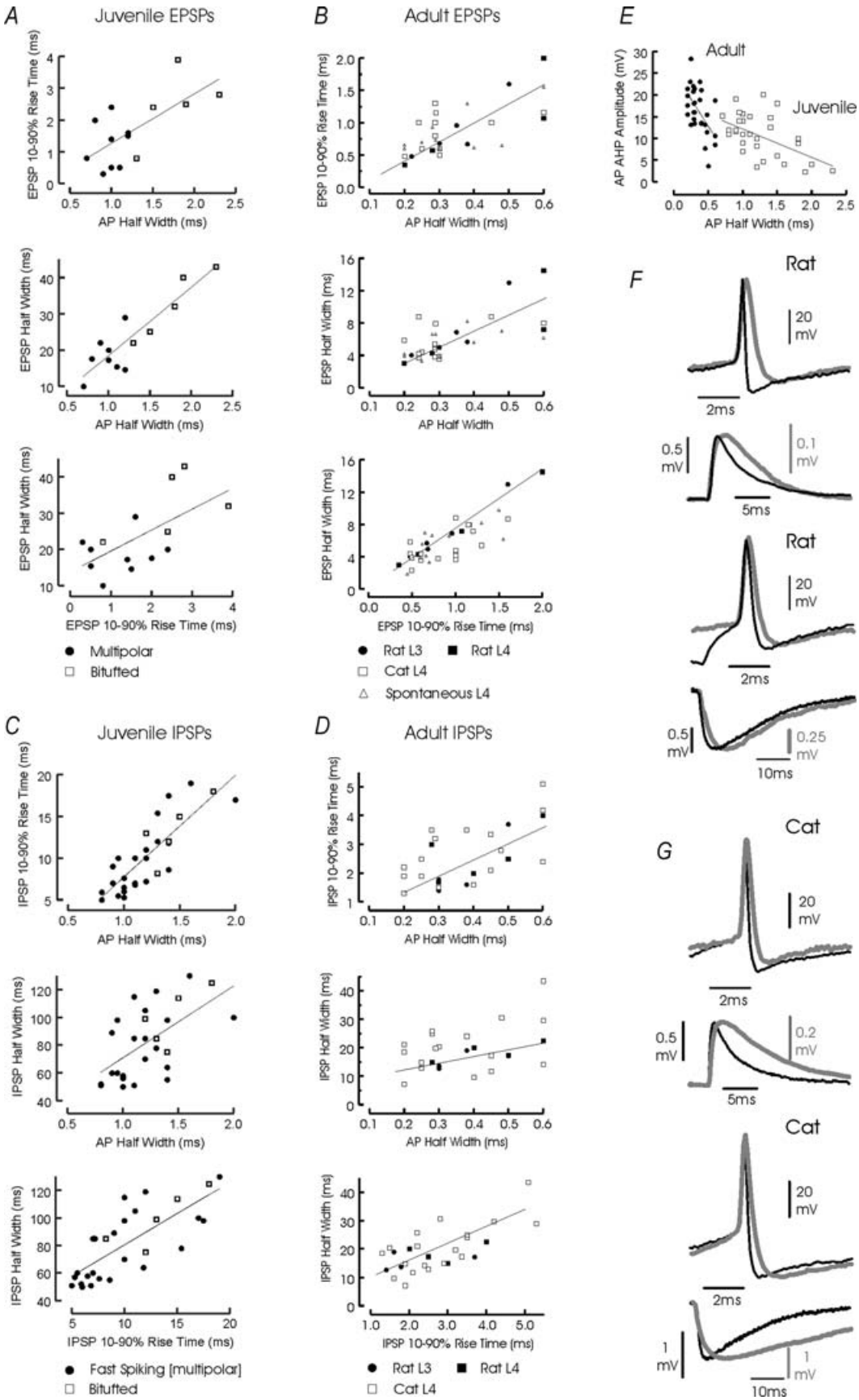

and whether they are similar across species and at different stages of development, the properties of EPSPs elicited in interneurones and of the IPSPs they generated in spiny cells were plotted against the width at half-amplitude of the interneurone AP. Interneurone AP duration was the single characteristic that most clearly correlated with interneuronal morphology and immunofluorescent labelling for markers. Firing patterns were less tightly associated. Although continuous, non-adapting firing was seen predominantly in cells with narrow action potentials, adapting, stuttering and delayed firing were associated with a wider range of spike widths and morphologies.

Although considerable scatter was apparent, correlations between the AP width at half-amplitude and the EPSP and IPSP 10–90% rise times and widths at half-amplitude were found for both juvenile and adult connections (correlation coefficients ranged from 0.59 to 0.86; Fig. 1*A*–*D*). A negative correlation was also found between the AP width at half-amplitude and the depth of the AP-AHP in both juveniles and adults (correlation coefficients 0.53–0.71; Fig. 1*E*), i.e. the deeper the AP-AHP, the briefer the AP.

In Fig. 1*B*, *D* and *E*, the points obtained from adult rat and cat connections are plotted together (with different symbols), since no significant differences in the distributions of these parameters, nor in the correlations between them was found. In striking contrast, despite similar relationships between parameters, all time scale measures obtained from juvenile connections were broader than the equivalent parameter for either adult rat or cat connections and most of the distributions did not overlap. Action potentials, EPSPs and IPSPs were significantly narrower in adult tissue, and AP-AHPs were significantly deeper ($P < 0.01$ to $P < 0.0000005$, Student's unpaired *t* test).

Comparison of the maximum and minimum values and the means and medians for each population showed that juvenile events were consistently between 3.5 and 4.5 times slower than equivalent adult events, with the exception of EPSP 10–90% rise time. For this parameter, juvenile measures exhibited a wider relative distribution, with the fastest events parallelling those in the adult and the slowest having four times the duration, with mean and median values twice as long as in the adult (2.1 and 1.9). This may suggest that the maximal rate of rise in adult interneurones is limited by the passive properties of the neurones.

Complex relationships between interspike interval and EPSP amplitude

Fast EPSPs in multipolar cells with narrow spikes consistently demonstrated paired pulse and frequency-dependent depression in both juvenile rats and adult rats and cats (Figs 2, 4 and 6), while slow EPSPs in bitufted cells exhibited facilitation (Figs 3, 5 and 7), as previously described (Thomson *et al.* 1993, 1995; Buhl *et al.* 1997; Galarreta & Hestrin, 1998; Markram *et al.* 1998; Reyes *et al.* 1998; Wang *et al.* 2002, 2004; Beierlein *et al.* 2003). In juvenile slices, the depression typical of EPSPs recorded in multipolar interneurones can be seen in Fig. 2 and the facilitation typical of EPSPs recorded in bitufted interneurones in Fig. 3.

Previous studies in adult slices have demonstrated that facilitation at inputs onto interneurones in layer 6 (West *et al.* 2006) and depression at a number of different types of cortical pyramid–pyramid and pyramid–interneurone synapses (Thomson, West, 2003; Bannister & Thomson, 2006) do not necessarily decay with a simple exponential relationship between interspike interval and EPSP amplitude. To investigate this in the present study, EPSPs were activated over a range of

Figure 1. Correlations between the AP width at half-amplitude and the time course of EPSPs and IPSPs associated with different classes of interneurones
In *A* and *B*, the 10–90% rise time of the EPSP (top) and the EPSP width at half-amplitude (half-width, middle) are plotted against the AP half-width and below, the EPSP half-width is plotted against EPSP rise time for juveniles (*A*) and adults (*B*). Similar plots for juvenile and adult IPSPs are shown in *C* and *D*. In *A* and *C*, measurements from multipolar juvenile interneurones are indicated by the filled circles and those from bitufted interneurones by the open circles. In *B* and *D*, adult rat measurements from all interneurones included in this study are shown as filled and adult cat measurements as open symbols. The regression lines were fitted to all juvenile rat data (*A* and *C*) and to adult rat data (*B* and *D*) for direct comparison. In *E*, the width at half-amplitude of the AP-AHP is plotted against the AP half-width for juvenile (open symbols) and adult interneurones (closed symbols). In *F* (adult rat) and *G* (cat), examples of interneuronal APs elicited with threshold depolarizations and of averaged EPSPs elicited in and IPSPs elicited by these interneurones are shown below superimposed for comparison. In each case, the narrower AP and associated PSP is shown by the thinner black lines and the broader AP and associated PSP by the thicker grey lines. Note that the time scales for APs and EPSP/IPSPs are different. The correlation coefficients for the plots are as follows: adult AP HW *versus* EPSP RT, 0.96; AP HW *versus* EPSP HW, 0.82; AP HW *versus* IPSP RT, 0.58; AP HW *versus* IPSP HW, 0.58; EPSP RT *versus* EPSP HW, 0.88; IPSP RT *versus* IPSP HW, 0.73; AP HW *versus* AHP amplitude, 0.88; juvenile AP HW *versus* EPSP RT, 0.68; AP HW *versus* EPSP HW, 0.90; AP HW *versus* IPSP RT, 0.83; AP HW *versus* IPSP HW, 0.59; EPSP RT *versus* EPSP HW, 0.63; IPSP RT *versus* IPSP HW, 0.76; and AP HW *versus* AHP amplitude, 0.60.

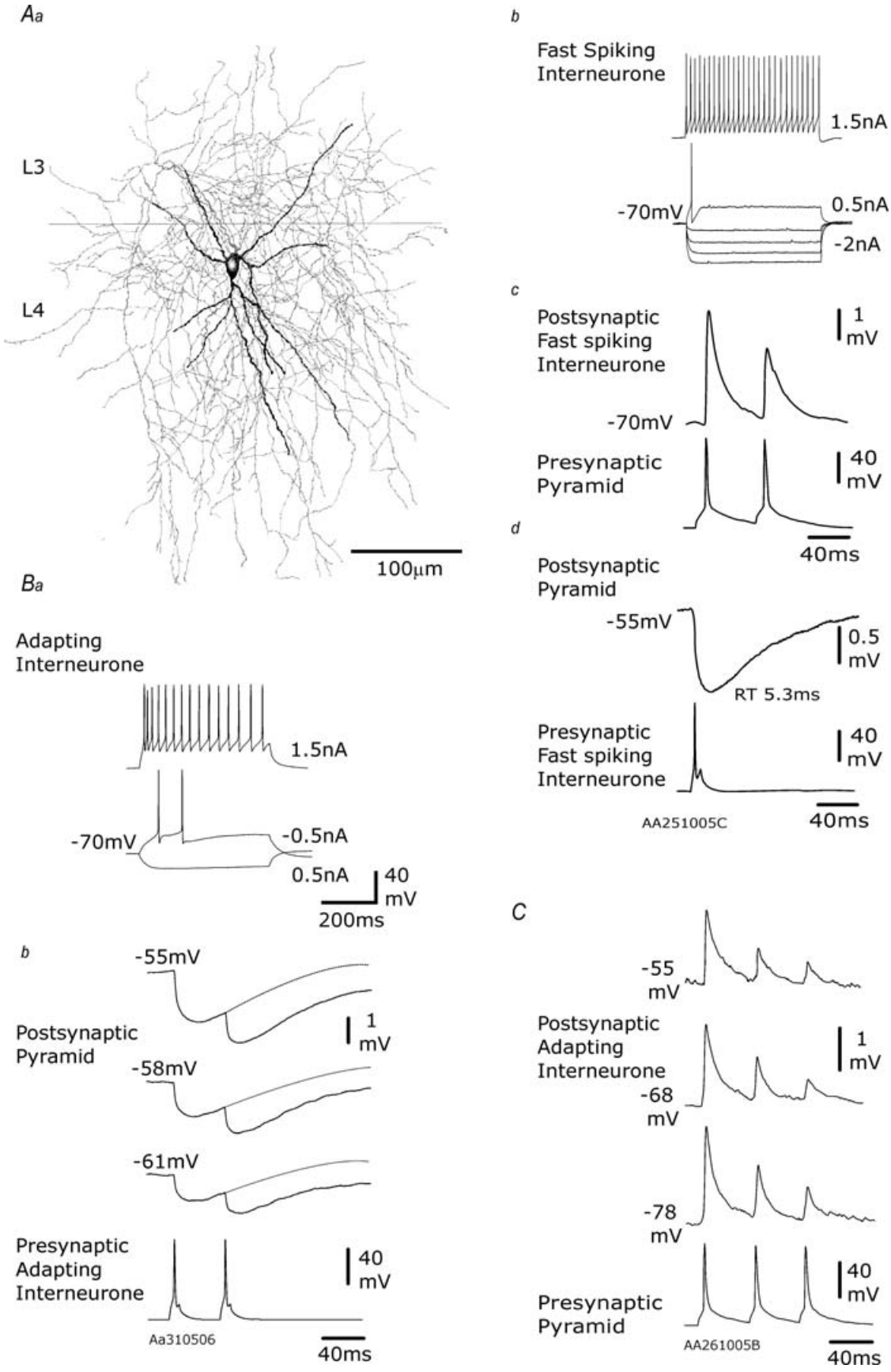

interspike intervals. The results of analysis are illustrated in Figs 5, 6 and 7, using three different approaches. Firstly, averaged second, third, etc. EPSPs were generated for presynaptic spike pairs or trains in which the firing pattern was identical. The composite averages are shown colour coded according to the average amplitude of the second, third or later EPSPs in trains. Secondly, EPSP amplitude was plotted against the interspike interval that immediately preceded it, as a two-dimensional plot. Thirdly, the influence of both first EPSP amplitude and interspike interval on second EPSP amplitude and the combined effects of the first and second intervals on the third EPSP amplitude are explored with three-dimensional plots rendered as colour contours.

Many previous studies of the dynamic properties of synapses have focused on those mechanisms whose strength appears to be inversely related to the release probability at the time of the first AP and which are proposed to decay exponentially. These are mechanisms such as release-dependent depression, which has its most pronounced functional impact at short interspike intervals when release probability is high, and facilitation, with its most pronounced impact at short intervals when release probability is very low (for review see Thomson, 2003). Recovery from depression or facilitation that does not follow a monotonic decay has been suggested to result from coexpression of both of these forms of short-term plasticity, and a range of more complex time courses are predicted to result if their power and decay rates are significantly different (Tsodyks & Markram, 1997).

In the present study, depression and facilitation rarely followed a simple exponential decay and were not always most pronounced at the shortest intervals. This is illustrated for three different types of connection in Figs 5–7. In the pyramid–bitufted cell pair illustrated in Fig. 5, the two-dimensional plots of second to sixth EPSP amplitudes against interspike interval (Fig. 5*H*) demonstrate that although facilitation/augmentation was apparent at all intervals tested, it was not maximal at the shortest intervals. It increased further between 10 and 20 ms with second EPSPs and between 20 and 40 ms for later EPSPs. Third and fourth EPSPs showed complex relationships with the preceding intervals, such that average EPSP amplitude was not determined solely by the immediately preceding interval (Figs 5*C–F*), nor by the sum of the preceding intervals, but by some more complex relationship between them. In the large, multipolar parvalbumin immunopositive interneurone illustrated in Fig. 6, the second EPSP depression recovered rapidly at first, but did not thereafter exhibit a smooth decay. Mild facilitation and depression alternated at longer intervals. From the composite averages and both the two- and three-dimensional plots (Fig. 6*D–F*), third EPSP amplitude can again be seen to vary depending upon a complex relationship between both preceding intervals. In the facilitating pyramid–Martinotti cell pair illustrated in Fig. 7, simple two-dimensional plots of second and third EPSP amplitude against interspike interval indicate an approximately exponential decline in amplitude with increasing intervals, but with peaks and troughs superimposed. When the first interspike interval remained constant and the second interval was varied, the average third EPSP was not always largest when preceded by a short second interval or smallest when it followed a long second interval (Fig. 7*C* and *D*). Unlike the connection in Fig. 5, this EPSP exhibited no augmentation and, indeed, with some patterns of presynaptic firing later EPSPs in trains were depressed (relative to first EPSPs), particularly at intervals around 20 ms (Fig. 7*G*).

Depression and facilitation of EPSPs are mediated presynaptically

Failures of transmission were apparent in four cat, three adult rat and 11 juvenile rat depressing connections and in two cat, three adult rat and seven juvenile rat facilitating connections. In both adult and juvenile connections, facilitation/augmentation was associated with a decrease and depression was associated with an increase in the proportion of apparent failures of transmission (Supplementary Fig. 6*B*). In a Binomial model for release, in which n is the number of release sites, p the probability of release and q the quantal amplitude, the inverse square of the coefficient of variation $CV^{-2} = [np/(1-p)]$ and the mean EPSP amplitude, $M = npq$. In the majority of cases, the proportional change in CV^{-2} was greater than the proportional change in M. These findings indicate that both facilitation/augmentation and depression were mediated predominantly presynaptically and by a change in release probability, p (Supplementary Fig. 6*A*) in both juvenile and adult tissue.

Figure 2. EPSPs and IPSPs elicited in juvenile layer 4 multipolar interneurones
In *Aa*, a multipolar interneurone reconstruction is illustrated (dendrites black, axon grey). The firing pattern of this interneurone is shown in *Ab* and its reciprocal connections with a simultaneously recorded spiny cell in *Ac* and *Ad*. In *Ac*, the paired pulse depression typical of fast excitatory inputs onto multipolar interneurones is illustrated, and in *Ad* the fast IPSP that this interneurone elicits in its pyramidal partner is shown. In *B* and *C*, recordings from two further multipolar interneurones that had fast APs but adapting firing patterns (*Ba*) are shown. The IPSP elicited by one of these cells with an extrapolated reversal potential of −69 mV and exhibiting paired pulse depression is shown in *Bb*. The fast, depressing EPSP elicited in another is shown in *C*. In each case, the presynaptic recording is a single sweep and the postsynaptic an average of 20–50 sweeps.

Significance of peaks and troughs in plots of EPSP amplitude against insterpike interval

Although the averaged EPSP records and the smoothed plots demonstrate trends, these connections displayed high coefficients of variation. Therefore, to determine whether the peaks and troughs apparent in the two-dimensional plots of EPSP amplitude against interspike interval and those in the three-dimensional plots of third EPSP amplitude against first and second

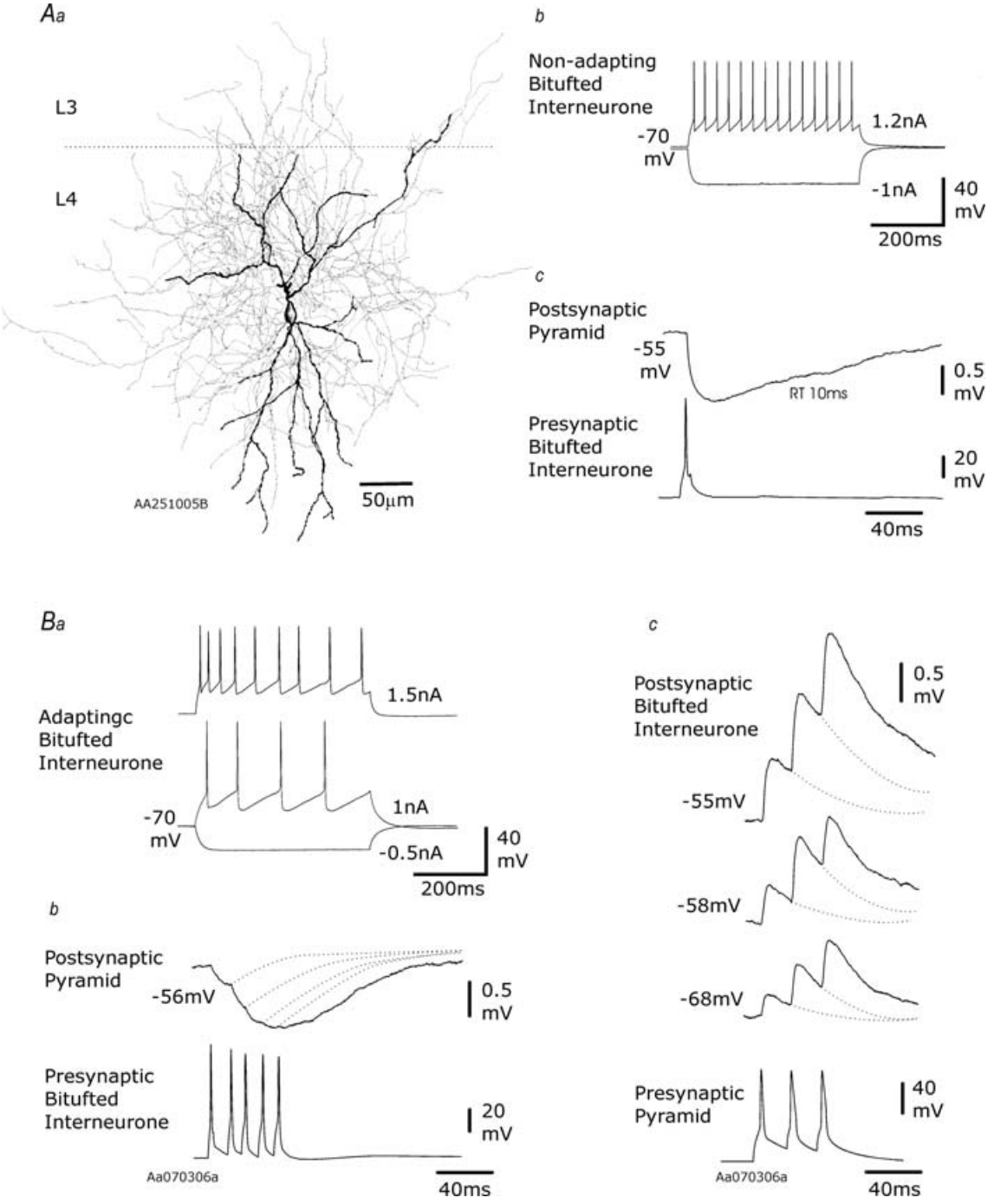

Figure 3. EPSPs and IPSPs elicited in juvenile layer 4 bitufted interneurones
In *Aa*, a bitufted interneurone reconstruction is illustrated (dendrites black, axon grey). The non-adapting firing pattern of this interneurone is shown in *Ab* and the slow IPSP it elicits in a spiny cell in *Ac*. In *B*, recordings from another bitufted interneurone that had broad APs and an adapting firing pattern (*Ba*) are shown. The IPSP elicited by one of these cells in a simultaneously recorded pyramidal cell exhibited modest paired pulse facilitation, but no augmentation (*Bb*). The slow, facilitating EPSP elicited by the reciprocally connected pyramid is shown in *Bc*. In each case, the presynaptic recording is a single sweep and the postsynaptic an average of 20–50 sweeps.

interspike interval were significant, analysis of variance and pairwise unpaired Student's *t* tests were performed (see Methods). Data subsets that represented the peaks and troughs were selected and compared in six paired recordings.

Significant differences between mean EPSP amplitudes in these subsets were indicated by analysis of variance ($P = 0.0001$–0.0009 for two-dimensional second and third EPSP plots; $P = 0.0002$–0.047 for three-dimensional plots of third EPSPs; one way ANOVA). Subsets that corresponded to successive peaks, or to successive troughs in two-dimensional plots were not found to be significantly different ($P > 0.05$ pairwise unpaired Student's *t* tests), but the means of data subsets that corresponded to a peak and the preceding or following trough differed significantly

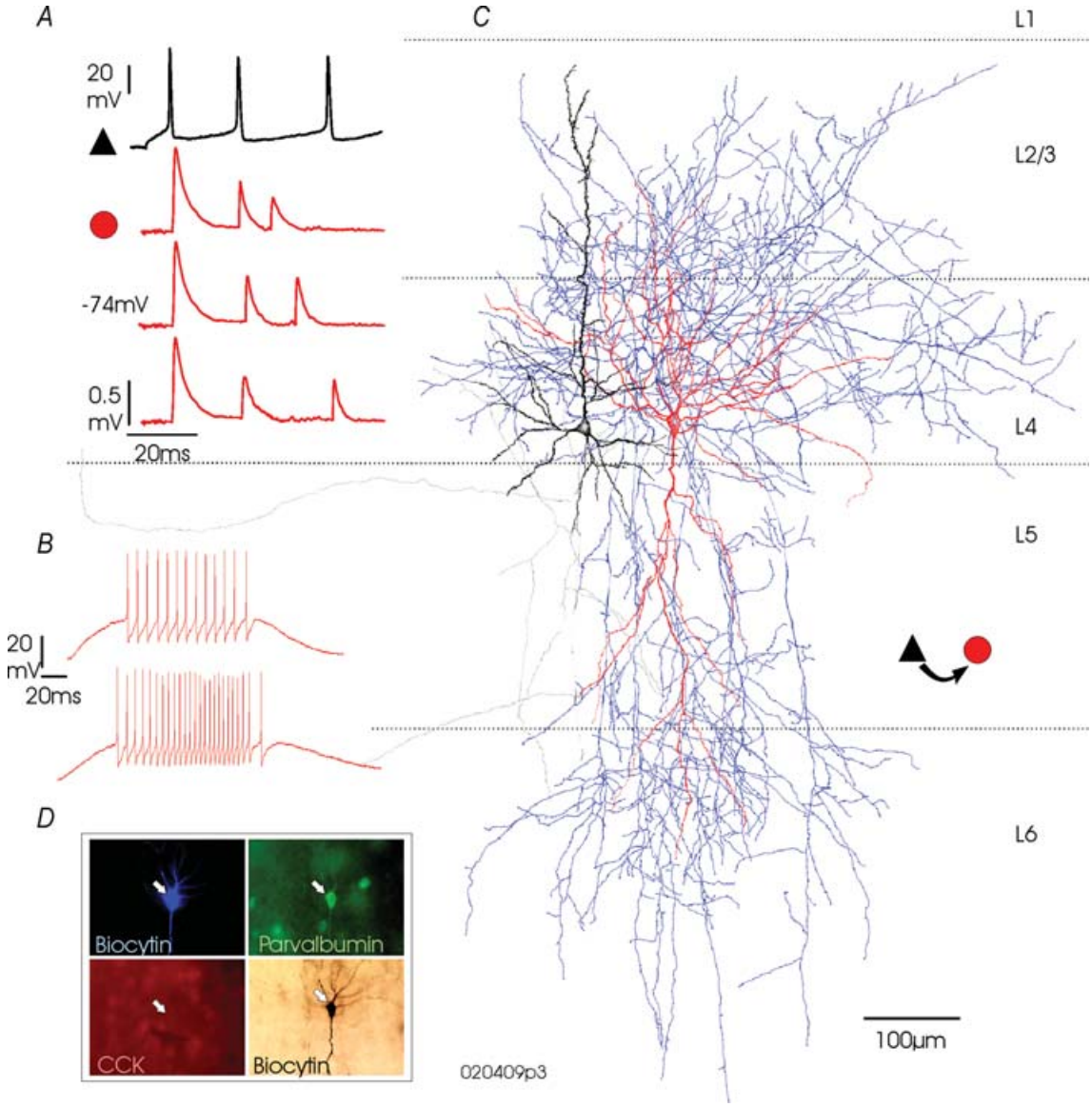

Figure 4. EPSPs elicited in a large multipolar parvalbumin-immunopositive interneurone by a simultaneously recorded pyramidal cell in adult rat somatosensory cortex
In *A*, the fast, depressing EPSPs elicited in this interneurone by a simultaneously recorded pyramid are illustrated. Responses to three different firing patterns are shown. The presynaptic pyramidal recording is a single sweep and the postsynaptic records are composite averages including 20–50 sweeps per component. In *B*, the continuous firing that could be elicited in this stuttering/stopping interneurone when a gradually increasing ramped current pulse was applied is shown. The reconstruction of this layer 4 interneurone shows the partly myelinated axon (blue) and dendrites (red) extending into layers 3 and 6, with significant axonal arborization in layers 3, 4 and 6. The presynaptic pyramid is drawn in black (axon grey). The immunofluorescent identification of parvalbumin (green) in this biocytin-labelled cell (blue fluorescence; black, HRP) and the absence of cholecystokinin (CCK, red) are shown in *D*.

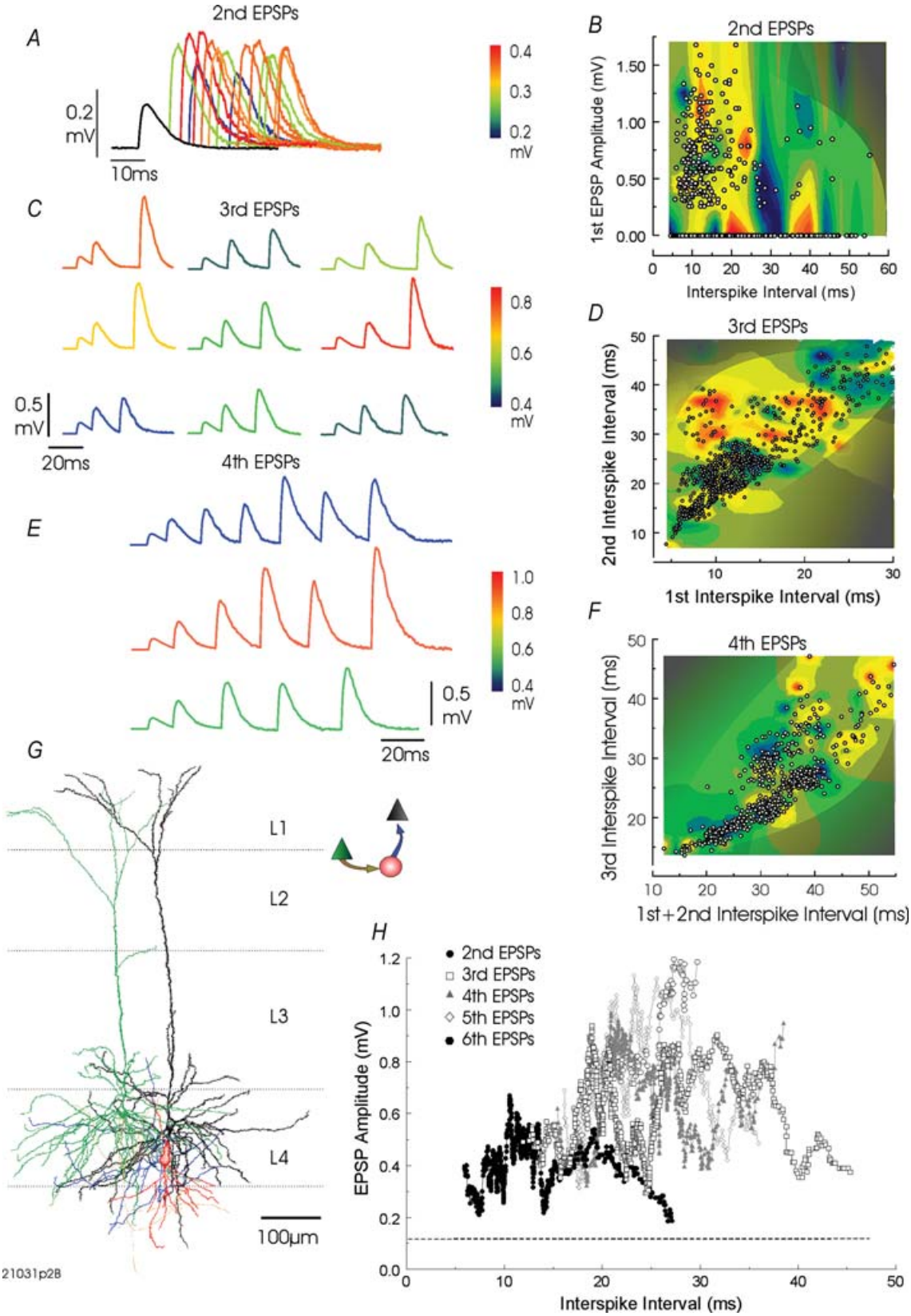

Table 1. Action potential width at half-amplitude (AP HW), EPSP and IPSP amplitude, 10–90% rise time (RT) and width at half-amplitude (HW) for connections made by interneurones in juvenile rat and in adult rat and cat neocortex

Type of interneurone	AP HW (ms)	EPSP hit rate	EPSP amplitude (mV)	EPSP RT (ms)	EPSP HW (ms)	IPSP hit rate	IPSP amplitude (mV)	IPSP RT (ms)	IPSP HW (ms)
Rat juvenile, layers 3–5									
Multipolar (32): 12 EPSPs, 23 IPSPs, 3 reciprocal	1.07 ± 0.19*†	1/1	0.94 ± 0.7*†	1.6 ± 1.2*†	20 ± 5.7*†	1/3	0.57 ± 0.55*	9.4 ± 3.8*†	75.2 ± 19.8*†
Bitufted (12): 9 EPSPs, 7 IPSPs, 4 reciprocal	1.67 ± 0.33	1/4	0.21 ± 0.16*†	3.8 ± 1.9*†	29 .1 ± 10.3*†	1/3	0.86 ± 0.43*†	14 ± 3.9*†	110 ± 18*†
Rat adult, layers 3–4									
FS (8): 7 EPSPs, 4 IPSPs, 2 reciprocal	0.27 ± 0.04	1/10	2.4 ± 1.94†	0.52 ± 0.14†	4.1 ± 0.82†	1/9	1.0 ± 0.41†	1.97 ± 0.70	13.8 ± 0.94†
Non-FS (9): 7 EPSPs, 5 IPSPs, 3 reciprocal	0.48 ± 0.11	1/4	1.36 ± 0.87	1.26 ± 0.53	9.5 ± 3.9	1/7	1.26 ± 0.45	2.76 ± 1.05	19.2 ± 2.2
Cat Adult, layer 4									
FS (17): 11 EPSPs, 10 IPSPs, 4 reciprocal	0.26 ± 0.03	1/14	2.7 ± 1.6†	0.76 ± 0.27†	5.0 ± 1.8†	1/6.4	1.1 ± 0.71†	2.1 ± 0.77†	17.1 ± 6.8
Non-FS (9): 3 EPSPs, 10 IPSPs, 4 reciprocal	0.48 ± 0.09	1/7	1.5 ± 1.3	1.2 ± 0.30	8.2 ± 0.72	1/4	1.25 ± 0.91	3.32 ± 1.23	22.5 ± 10.7

The juvenile interneurones were classified broadly as either mutipolar or bitufted. Since the adult interneurones exhibited a wide range of morphological features, these interneurones were classified according to their AP width at half-amplitude (fast spiking (FS), AP HW $\leq$ 0.3 ms; and non-FS, AP HW $>$ 0.3 ms). Values are means ± S.D. The parameters for which the means were significantly different between the juvenile and the adult populations are indicated by * ($P < 0.03$). The parameters for which the means were significantly different between the two populations from the same age and species are indicated by † ($P < 0.05$). Numbers in parentheses indicate the number of cells included.

($P < 0.05$ to $P < 1 \times 10^{-5}$; 7, 6 and 5 tests per pair for those illustrated in Figs 5, 6 and 7, respectively). When these comparisons were subjected to more rigorous testing (Bonferroni correction), only those multiple comparisons corresponding to the more pronounced peaks and troughs, each represented by >30 single sweep measurements reached significance ($P < 0.05$; 3, 5 and 3 pairwise unpaired tests per pair, respectively). Intervals between successive peaks or successive troughs varied between 8 and 22 ms (mean 12 ± 4 ms).

For the three-dimensional plots, pairwise unpaired *t* tests demonstrated that the levels of significance for data subsets that were widely different in colour, e.g. blue and orange, were higher ($P = 0.0001$–0.02) than where the colour difference was intermediate, e.g. dark blue to green, or yellow to red ($P = 0.01$–0.04). For subsets with similar colours, e.g. dark and light blue, or yellow and light green, the differences in the means were not significant ($P > 0.05$).

EPSP paired pulse ratios correlate with interneuronal firing properties

Juvenile connections were not subjected to detailed studies of the time course of synaptic depression or facilitation at short interspike intervals because the long duration of the EPSPs confounded detailed analysis at short intervals. Fixed interspike intervals, typically of 50 ms, were studied. To compare the dynamic properties across age groups, therefore, the paired pulse ratio was plotted against AP width at half-amplitude (Fig. 8). Strong correlations were found (correlation 0.68–0.95), with the slope of the linear regression decreasing and the intercept becoming less negative with increasing intervals in both adult rat and cat connections (for clarity in Fig. 8*A*, only one regression line is shown, calculated for the whole adult population). The plots in Supplementary Fig. 6*C*–*F* illustrate the relationships between paired pulse ratio and EPSP rise time and EPSP width at half-amplitude. They show that

Figure 5. Facilitating and augmenting excitatory connections from a layer 4 pyramidal cell to a burst firing, bitufted interneurone in rat somatosensory cortex
In *A*, composite averages of responses to pairs of presynaptic APs at different interspike intervals demonstrate that second EPSPs are facilitated/augmented at all interspike intervals tested, but not maximally at the shortest intervals. In addition, peaks and troughs are superimposed on a gradual increase then a decrease in EPSP amplitude. This is also apparent from the plots in *B* and for second to sixth EPSPs in *H*. In *B*, second EPSP amplitude is plotted against first interspike interval and first EPSP amplitude as a three-dimensional plot rendered as a colour contour. The effect of interspike interval can be seen to dominate. The composite averages shown in *C* and *E* and the three-dimensional plots in *D* and *F* demonstrate that third (*C* and *D*) and fourth (*E* and *F*) EPSP average amplitude is determined by complex relationships between preceding interspike intervals, neither the preceding interval nor the sum of all preceding intervals alone determining the amplitude of the next EPSP. Composite averages are colour coded according to the amplitude of the averaged second (*A*) third (*C*) and fourth EPSPs (*E*), respectively. *G*, this interneurone, which was only partly recovered (red dendrites, blue axon and green presynaptic pyramid dendrites) was also presynaptic to another layer 4 pyramid (drawn in black; IPSPs not illustrated).

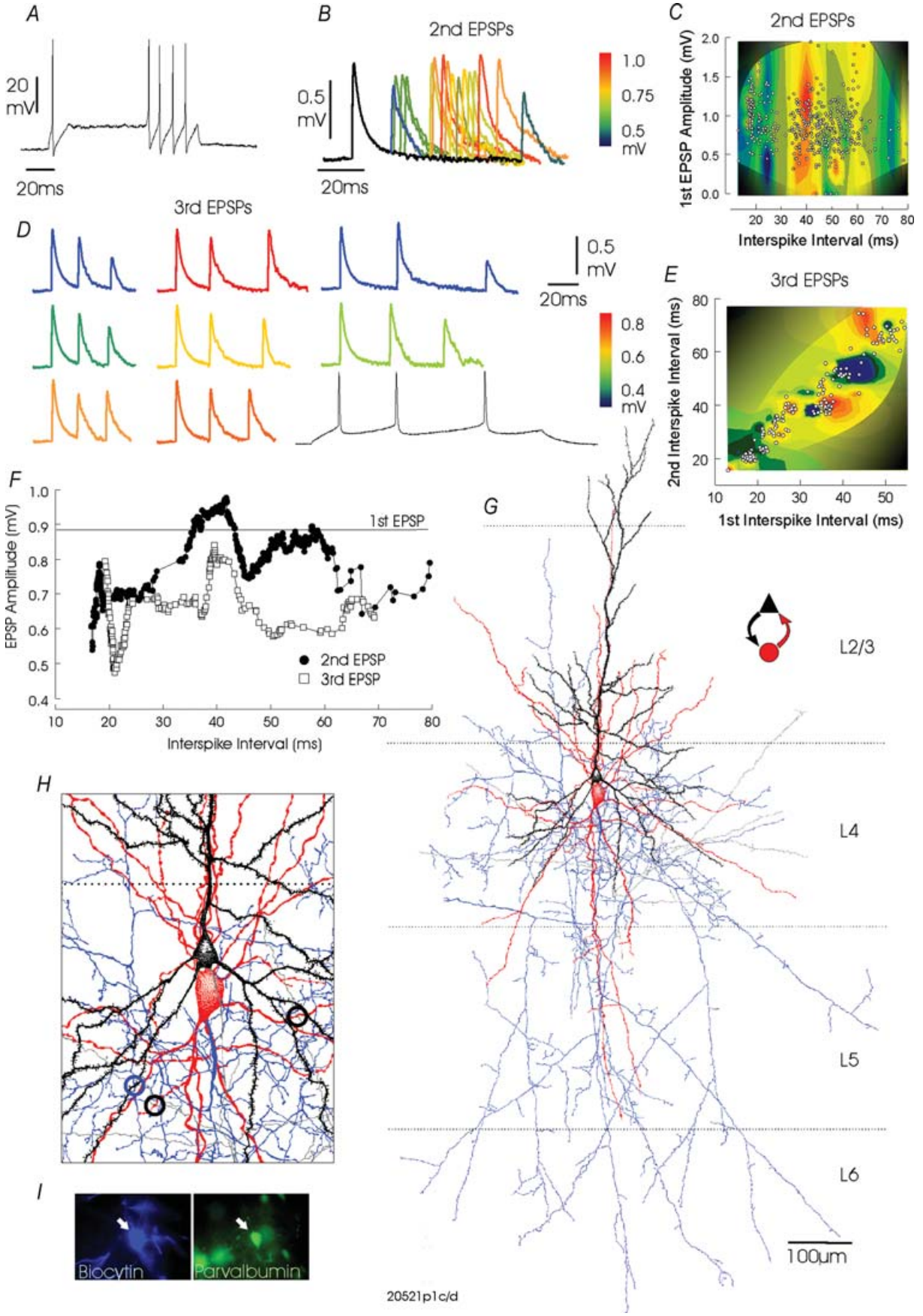

EPSPs with brief rise times and widths at half-amplitude demonstrate depression and that the connections that demonstrate facilitation generally have a slow time course.

In both juvenile and adult slices, multipolar interneurones with narrow spikes consistently received narrow depressing EPSPs, while bitufted, adapting and burst firing interneurones received broad facilitating EPSPs, as reported previously in juvenile layer 4 interneurones (Beierlein *et al.* 2003). There was only one exception to this correlation. This was an adult cat bipolar interneurone with a broad AP (0.6 ms) a stuttering/stopping firing pattern, broad IPSPs (width at half-amplitude of 43.5 ms), but in which the broad EPSPs (half-width 8 ms) demonstrated depression (see star in Fig. 8*A* and Supplementary Fig. 5). This is consistent with previous reports that bipolar interneurones receive depressing inputs (Porter *et al.* 1998; Rozov *et al.* 2001). In both adults and juveniles, the EPSPs that facilitated were significantly smaller in response to the first AP (0.49 ± 0.18 and 0.21 ± 0.19 mV, respectively) than those that depressed (1.42 ± 0.96 and 0.93 ± 0.69 mV, respectively; $P < 0.05$, Student's unpaired t test). These relationships are consistent with evidence that facilitating EPSPs have a low release probability (Deuchars & Thomson, 1995; Thomson *et al.* 1995; Markram *et al.* 1998; Wang *et al.* 2002, 2004) and, indeed, the proportion of apparent failures of transmission was higher for connections that facilitated.

Discussion

The major findings presented here are, firstly, the strong and similar correlations between interneuronal characteristics and the properties of the EPSPs they receive and of the IPSPs that they generate in two species and in two different age groups and, secondly, that the durations of both interneuronal APs and of their EPSPs and IPSPs were considerably longer in juveniles at 20°C than in adults at 35°C. Finally, detailed studies of the time course of facilitation and depression demonstrated that in adult connections neither decays with a smooth time course.

Correlations between firing characteristics and synaptic properties

In one comparison of synaptic connections made and received by two physiologically identified classes of interneurones in postnatal day 16–21 rats (fast spiking and low threshold spiking or LTS cells), both APs and EPSPs were briefer in fast spiking cells, though the IPSPs they elicited were not reported to be significantly different in time course (Beierlein *et al.* 2003). In postnatal day 12–15 rats, only the IPSC rise time, not its decay, was longer in LTS cells (Xiang *et al.* 2002). The findings presented here demonstrate for the first time that data obtained from one age group using one recording technique can predict in another age group, studied with a different technique, parameters such as AP half-width and AP-AHP amplitude, EPSP and IPSP time course and degree of facilitation or depression and the correlations between them.

Slower time course of events in juvenile slices recorded at 20°C

Juvenile (postnatal day 18–22) APs and synaptic events at 20°C were approximately four times slower in the present study than in adults at 35°C. That the temperature contributes significantly is suggested when comparisons are made with a previous study on postnatal day 14–21 rat slices at 32°C (Beierlein *et al.* 2003).

Figure 6. Depressing excitatory connections from a layer 4 pyramidal cell to a narrow spike, stuttering, parvalbumin-immunopositive multipolar interneurone in cat visual cortex
The stuttering firing pattern of this interneurone in response to a suprathreshold depolarizing pulse is shown in *A*. In *B*, composite averages of responses to pairs of presynaptic APs at different interspike intervals demonstrate that second EPSPs do not exhibit a smooth recovery from paired pulse depression. Peaks and troughs are apparent in the decay and result in modest facilitation between 35 and 42 ms. This can also be seen in the three-dimensional plot in *C*, in which second EPSP amplitude is plotted against first interspike interval and first EPSP amplitude as a three-dimensional plot rendered as a colour contour, and in *F*, where second and third EPSP amplitudes are plotted against interspike interval. The complex relationship between third EPSP amplitude and the two preceding interspike intervals can be seen in the composite averages in *D* and the three-dimensional plot in *E*. In *D*, a single presynaptic sweep is also illustrated. In *B*, traces are colour coded according to the average second EPSP amplitude and in *D* according to the average third EPSP amplitude. The reconstruction of this interneurone and the pyramidal cell with which it was reciprocally connected is shown in *G*. The interneurone dendrites are drawn in red and its axon in blue. The interneuronal dendrites extended into layers 3 and 5 and its axon ramified largely adjacent to and below the soma and extended throughout layers 4, 5 and 6, projecting weakly into layer 3. The pyramid which was reciprocally connected to the interneurnone is drawn in black and its axon in grey (IPSPs not illustrated). In *H*, a portion of the reconstruction is shown at higher magnification to illustrate points of close membrane apposition between the interneurone axon and a secondary basal pyramidal dendrite (blue open circle) and between the pyramidal axon and two secondary interneuronal dendrites (black open circles). The immunofluorescent labelling of parvalbumin (green) in this interneurone is shown in *I*.

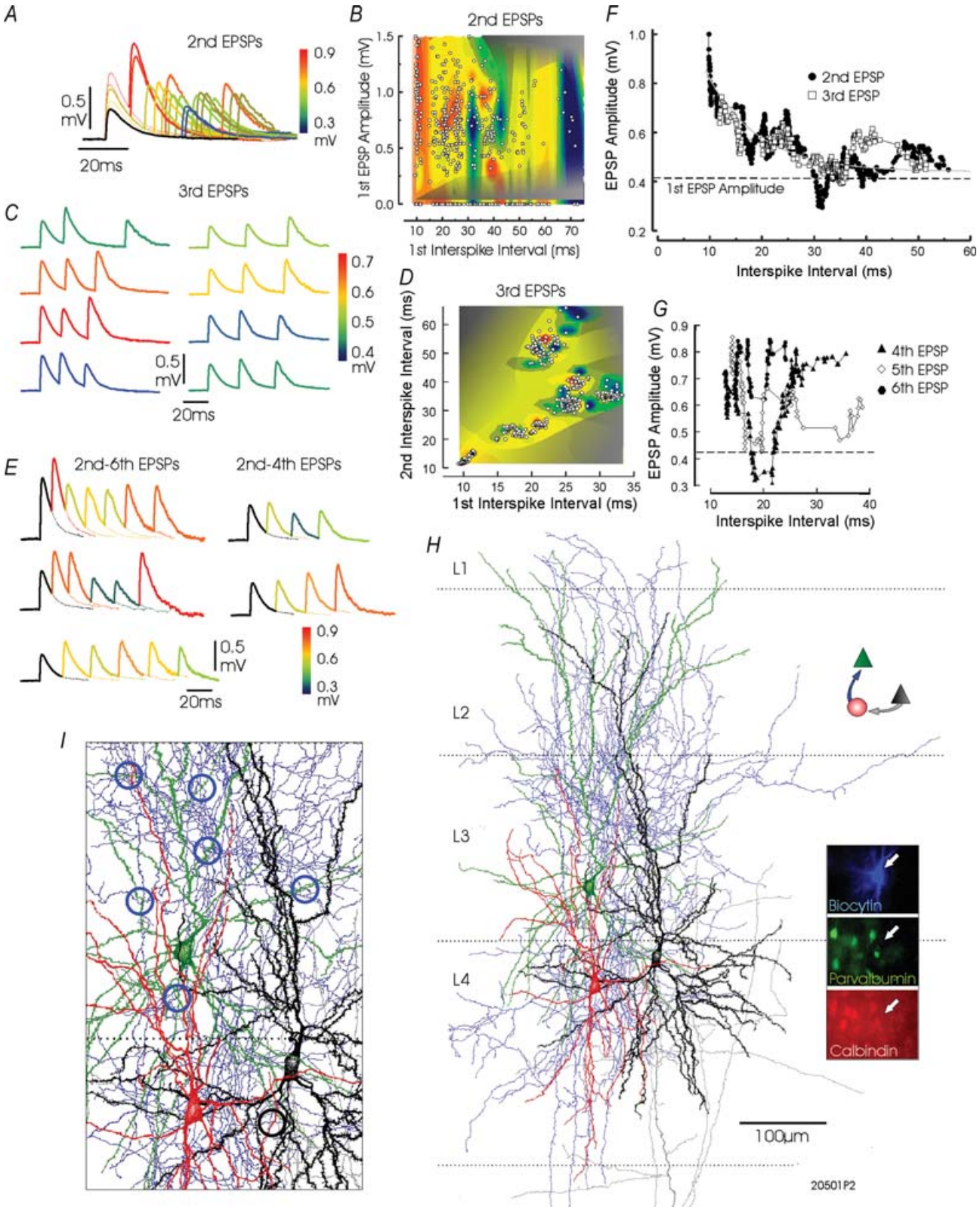

From the measurements given there, only AP width at half-amplitude was slower than in the adult slices reported here. Indeed, the present adult populations include cells with broader APs, EPSPs and IPSPs than predicted by that previous study. These may represent a population of interneurones not investigated in that study, since the morphological characteristics of the interneurones were not described (Beierlein *et al.* 2003). In addition, DL-amino 5 phosphano valerate (AP5) was present throughout the experiments, which probably reduced the time course of their EPSPs. In younger (postnatal day 14–16) rats at 32–34°C, EPSPs were approximately twice as broad (Reyes *et al.* 1998) as in adult or postnatal day 14–21 slices (Beierlein *et al.* 2003).

The increasing speed of events during development and with temperature parallels a decrease in membrane time constants; from 14 to 20 ms in nest basket cells (Wang *et al.* 2002) and 20–24 ms in Martinotti cells at postnatal day 13–15 (Wang *et al.* 2004) to 8.8 ms in fast spiking and 16.4 ms in LTS cells at postnatal day 14–21 (Beierlein *et al.* 2003) and finally to 5 ms in adult multipolar interneurones with narrow spikes (< 0.3 ms) and 9 ms in bitufted cells (including Martinotti cells) with broader spikes. At the lower temperature, time constants at postnatal day 18–22 were longer, being 22 ms in multipolar cells with narrow spikes and 28 ms in bitufted cells, again approximately four times the duration of membrane time constants in adult interneurones at 35°C. A reasonable explanation is that a threefold increase in rate results from the 15°C difference in temperature, while a twofold increase in rate occurs between postnatal day 13–16 and 18–22, with a smaller additional increase between postnatal day 18–22 and adult. The longer membrane time constants consistently reported for bitufted and LTS cells compared with multipolar narrow spike cells also correlate with the longer time course of EPSPs in these cells in all age groups, though it does not explain the longer time course of the IPSPs that they generate.

What is perhaps most compelling is the orchestrated way in which firing characteristics and synaptic potential durations speed up with increasing temperature and age, the properties of inputs and outputs remaining co-ordinated with firing properties. Thus, although it would be inappropriate to model adult activity *in vivo* based on the time course of events recorded from very young animals at room temperature, it may be reasonable to scale these properties according to the ratios found here.

Clearly, the functional characteristics of the different classes of interneurones remain similar from 2 weeks to 3 months (in rats), but how and why the adult cortex processes information on a faster time scale remains a conundrum. A simple explanation for this might be that there is a much greater need for the juvenile brain to be plastic and that mechanisms such as spike timing-dependent plasticity (Markram & Tsodyks, 1996) would be more readily activated with less tightly co-ordinated firing when EPSPs and IPSPs are broader. The negative correlation between AP half-width and AP-AHP amplitude supports previous findings that it is the strength and kinetics of this rectifying current that determine AP duration, spike accommodation and maximum firing frequency (Chen *et al.* 1996; Martina *et al.* 1998; Erisir *et al.* 1999; Chow *et al.* 1999; Kawaguchi & Kondo, 2002;

Figure 7. Facilitating excitatory connections from a layer 4 pyramidal cell to an adapting, parvalbumin-immunonegative bitufted Martinotti-like interneurone in cat visual cortex
In *A*, composite averages of responses to pairs of presynaptic APs at different interspike intervals demonstrate that second EPSPs do not exhibit a smooth recovery from paired pulse facilitation. Peaks and troughs are apparent in the decay. These are also apparent in the plot in *F*, to which a single exponential could be fitted (time constant 9.9 ms, correlation 0.83). The dominance of interspike interval over first EPSP amplitude in determining second EPSP amplitude can also be seen in the three-dimensional plot in *C*, in which second EPSP amplitude is plotted against first interspike interval and first EPSP amplitude as a three-dimensional plot rendered as a colour contour. Although when plotted against interspike interval (*F*) the decay of third EPSP amplitude against interval appears to parallel that of the second EPSP, a complex relationship between third EPSP amplitude and the two preceding interspike intervals can be seen in the composite averages in *C* and in the three-dimensional plot in *D*. The plots of fourth to sixth EPSP amplitudes against interspike intervals (*G*) demonstrate a pronounced 'notch' in the time course of recovery that results in the inconsistent facilitation seen in trains of EPSPs at some intervals (*E*). In *A*, traces are colour coded according to the average second EPSP amplitude, in *C* according to the average third EPSP amplitude and in *E* according to second-to-sixth EPSP amplitudes. The reconstruction of this interneurone and the pyramidal cells with which it was connected is shown in *H*. The interneurone dendrites are drawn in red and its axon in blue. The interneuronal dendrites extend through layers 4 and 3, and its axon ramifies adjacent to and above the soma in layers 4, 3/2 and 1. The presynaptic pyramid is drawn in black and its axon in grey, the postsynaptic pyramid in green (IPSPs not illustrated). In *I*, a portion of the reconstruction is shown at higher magnification to illustrate six points of close membrane apposition between the interneuronal axon and secondary, tertiary and quaternary dendrites of the postsynaptic pyramid (blue open circles), and between the pyramidal axon and one distal portion of a secondary interneuronal dendrite (black open circle). The immunofluorescent labelling of this slice, demonstrating that this cell was immunonegative for both parvalbumin (green) and calbindin (red), is shown in the inset in *H*.

Korngreen *et al.* 2005; Toledo-Rodriguez *et al.* 2005). Consistent with this, juvenile APs were broader and their AP-AHPs shallower than in adults. Without detailed analysis of channel type and density at different ages, we cannot predict whether it is subunit composition and/or channel density that changes with age. However, the faster membrane time constants possibly associated with the presence of high density voltage-gated channels with faster kinetics, plus the differential expression of glutamate receptor type 2 (GluR2) subunits (Angulo *et al.* 1997), may also contribute to the different durations of EPSPs between the age groups as well as in different types of interneurones.

Time course of synaptic depression and facilitation

Few studies in juvenile slices have attempted to investigate the time course of decay of facilitation or depression in any detail. It is not, therefore possible to draw direct comparisons with the present adult data. The general impression gained, however, is that in juveniles, both facilitation and depression are extremely powerful at interspike intervals at which many paired pulse effects have declined to low levels in adults (e.g. 50–100 ms), suggesting that the time course of changes in release probability may also be slower early in development.

Detailed analysis of adult EPSPs demonstrated that the complexity apparent in relationships between interspike intervals and EPSP amplitude reported previously in other types of connection (Thomson & West, 2003; West *et al.* 2006; Bannister & Thomson, 2006) is also apparent at connections received by layer 4 interneurones of several classes, whether the EPSP facilitated or depressed. The peaks and troughs in relationships between amplitude and interval appeared to be superimposed on several different combinations of more slowly changing events. For example, in connections that exhibited depression at short intervals, the peaks and troughs are superimposed on a more gradual, possibly exponential recovery (e.g. Fig. 6). Third and subsequent EPSPs were further depressed, but also exhibited complex recoveries. The degree to which these complex relationships influence circuit behaviour remains to be determined, but they resulted in large variations in average EPSP amplitude (20–75%) at around 80–90 Hz that appear to be time locked to the APs they follow. One interesting possibility is that this oscillation in release probability facilitates synaptic transfer and promotes synchrony at γ-frequencies when consecutive presynaptic APs coincide with peaks in population depolarization, but depresses transfer when the interspike interval is inappropriate.

Strongly facilitating connections exhibited two different underlying patterns which appeared to correlate with whether they also exhibited augmentation. In connections that exhibited strong augmentation (e.g. Fig. 5), second and subsequent EPSPs were not on average largest at the shortest intervals. Here the peaks and troughs are superimposed on a more a slowly increasing, then decreasing envelope. This could be explained by augmentation activated by a single preceding AP developing more slowly than facilitation, being cumulative over longer spike trains and resulting in greater amplification than facilitation alone. The overall effect is a gradually increasing amplitude over longer spike trains with a distinct, but non-linear frequency dependence (Fig. 5*E*). This gradual augmentation is the pattern most commonly reported for LTS interneurones in the previous studies cited above.

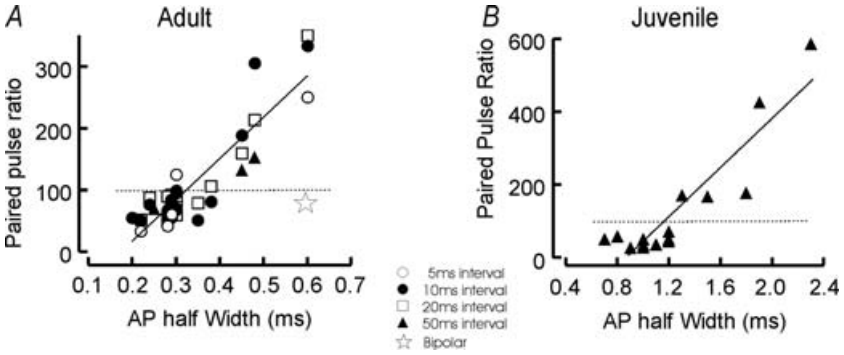

Figure 8. Correlation between EPSP paired pulse ratios and interneuronal AP width at half-amplitude
Adult (*A*) and juvenile measurements (*B*) are plotted. For juvenile EPSPs only interspike intervals of 50 ms were studied. For adult EPSPs a range of intervals is plotted (5, 10, 20 and 50 ms; see key for symbols). Linear regressions fitted to the data demonstrated strong correlations between paired pulse ratio and AP width at half-amplitude (correlation at 5 ms 0.68; at 10 ms 0.89; at 20 ms 0.93; and at 50 ms 0.95) with the slope becoming less steep (from 783% average amplitude per millisecond AP HW at 5 ms to 593% ms^{-1} at 50 ms) and the intercept less negative with increasing interspike intervals (from −147% at 5 ms to −93% at 50 ms). Only one regression line fitted to the complete adult data set is illustrated for clarity (adult correlation 0.91; juvenile 0.90). A single outlying point (* in *A*) represents the only bipolar interneurone in which EPSP paired pulse effects were studied (Supplemental Fig. 5) shown for an interval of 20 ms.

In contrast, in facilitating connections without strong augmentation (e.g. Martinotti cell, Fig. 7), the peaks and troughs are superimposed on a near exponential decline in second EPSP amplitude, and third EPSP dynamics parallel those of second EPSPs plotted in two dimensions. It is likely, therefore, that this decay represents facilitation in the absence of augmentation. A single exponential fit gave a time constant of 9.9 ms (correlation 0.83), again, very much briefer than that estimated for juvenile connections (Markram *et al.* 1998). Without augmentation and with pronounced troughs in the relationships between preceding interval and amplitude for later EPSPs in trains, a wide range of output patterns results. With some presynaptic firing patterns EPSP amplitude increased steadily, though not dramatically, during the train; with others it first declined, but increased again later in the train.

Conclusions

This is the first time that the significance of correlations between the duration of the AP and of the synaptic events elicited in and by interneurones and the degree of facilitation or depression has been demonstrated. These correlations underline the wide range of functions that cortical interneurones perform. Interneurones with narrow spikes and the ability to respond very rapidly receive EPSPs that depress powerfully. With their very brief duration, this precludes summation of successive EPSPs from one presynaptic cell and severely limits the time window within which convergent inputs can sum to threshold. Moreover, their output is also fast, ensuring that these cells either fire rapidly or not at all in response to a novel input and provide powerful, but brief, proximal inhibition of many neighbouring neurones, contributing to synchronization. At the other end of the spectrum are burst firing and adapting bitufted interneurones with broad APs. Neither these cells, nor their inputs can respond rapidly. Their broad, strongly augmenting EPSPs ensure that the inhibition they provide to pyramidal dendrites, though delayed in onset, will summate and be maintained for the duration of incoming spike trains. Between these two extremes are interneurones with intermediate properties. While it is clear that some distinct morphological subclasses can be identified (see Introduction) and that some interneuronal characteristics cluster in multidimensional space (e.g. Monyer & Markram, 2004; Toledo-Rodriguez *et al.* 2005), it is not yet possible to classify all subtypes of interneurones in neocortex. In the absence of a thorough classification, the correlations presented here provide a framework within which functional properties of interneurones can be assessed. The present study and comparisons with previous studies also demonstrate that although the time course of all events is slower early in development and is strongly affected by temperature, the way in which interneurones function within the circuit remains similar.

What is apparent is that the two neurones involved in a synaptic connection recognize each other and insert proteins/mechanisms appropriate for the cell on the 'other side' of the cleft. Thus, presynaptic boutons display transmitter release dynamics that correlate with the type of neurone that is postsynaptic to those boutons. Similarly, postsynaptic properties, such as IPSP time course and $GABA_A$ receptor subunit insertion (Thomson *et al.* 2000), correlate with the class of presynaptic interneurone. It is unlikely that the mechanisms that determine postsynaptic spike width are those that are directly signalled to the presynaptic or postsynaptic partners of each interneurone (to determine which pre- and postsynaptic proteins are inserted at each specific synapse). It is more likely that spike width is amongst the many characteristics determined by a cascade of genetically and environmentally determined factors that include the cell-to-cell signalling mechanisms that assist in this recognition process.

References

Ali AB & Nelson C (2006). Distinct Ca^{2+} channels mediate transmitter release at excitatory synapses displaying different dynamic properties in rat neocortex. *Cereb Cortex* **16**, 386–393.

Angulo MC, Lambolez B, Audinat E, Hestrin S & Rossier J (1997). Subunit composition, kinetic, and permeation properties of AMPA receptors in single neocortical nonpyramidal cells. *J Neurosci* **17**, 6685–6696.

Bannister AP & Thomson AM (2006). Dynamic properties of excitatory synaptic connections involving layer 4 pyramidal cells in adult rat and cat neocortex. *Cereb Cortex* [Epub ahead of print] DOI: 10.1093/cercor/bh/126.

Beierlein M, Gibson JR & Connors BW (2003). Two dynamically distinct inhibitory networks in layer 4 of the neocortex. *J Neurophysiol* **90**, 2987–3000.

Buhl EH, Tamas G, Szilagyi T, Stricker C, Paulsen O & Somogyi P (1997). Effect, number and location of synapses made by single pyramidal cells onto aspiny interneurons of cat visual cortex. *J Physiol* **500**, 689–713.

Cauli B, Audinat E, Lambolez B, Angulo MC, Ropert N, Tsuzuki K, Hestrin S & Rossier J (1997). Molecular and physiological diversity of cortical nonpyramidal cells. *J Neurosci* **17**, 3894–3906.

Chen W, Zhang JJ, Hu GY & Wu CP (1996). Different mechanisms underlying the repolarization of narrow and wide action potentials in pyramidal cells and interneurons of cat motor cortex. *Neuroscience* **73**, 57–68.

Chow A, Erisir A, Farb C, Nadal MS, Ozaita A, Lau D, Welker E & Rudy B (1999). K^+ channel expression distinguishes subpopulations of parvalbumin- and somatostatin-containing neocortical interneurons. *J Neurosci* **19**, 9332–9345.

Deuchars J & Thomson AM (1995). Innervation of burst firing interneurones by pyramidal cells in deep layers of rat somatomotor cortex: paired intracellular recordings with biocytin filling. *Neuroscience* **69**, 739–755.

Erisir A, Lau D, Rudy B & Leonard CS (1999). Function of specific K^+ channels in sustained high-frequency firing of fast-spiking neocortical interneurons. *J Neurophysiol* **82**, 2476–2489.

Galarreta M & Hestrin S (1998). Frequency-dependent synaptic depression and the balance of excitation and inhibition in the neocortex. *Nat Neurosci* **1**, 587–594.

Gupta A, Wang Y & Markram H (2000). Organizing principles for a diversity of GABAergic interneurons and synapses in the neocortex. *Science* **287**, 273–278.

Houser CR, Vaughn JE, Hendry SHC, Jones EG & Peters A (1984). GABA neurons in the cerebral cortex. In *Cerebral Cortex: Functional Properties of Cortical Cells*, ed.Peters A & Jones EG, pp. 63–87. Plenum Press, New York.

Hughes DI, Bannister AP, Pawelzik HP & Thomson AM (2000). Double immunofluorescence, peroxidase labelling and ultrastructural analysis of interneurones following prolonged electrophysiological recordings *in vitro*. *J Neurosci Meth* **101**, 107–116.

Jones EG (1975). Varieties and distribution of non-pyramidal cells in the somatic sensory cortex of the squirrel monkey. *J Comp Neurol* **160**, 205–267.

Kawaguchi Y & Kondo S (2002). Parvalbumin, somatostatin and cholecystokinin as chemical markers for specific GABAergic interneuron types in the rat frontal cortex. *J Neurocytol* **31**, 277–287.

Kawaguchi Y & Kubota Y (1993). Correlation of physiological subgroupings of nonpyramidal cells with parvalbumin- and calbindinD28k-immunoreactive neurons in layer V of rat frontal cortex. *J Neurophysiol* **70**, 87–96.

Kawaguchi Y & Kubota Y (1996). Physiological and morphological identification of somatostatin- or vasoactive intestinal polypeptide-containing cells among GABAergic cell subtypes in rat frontal cortex. *J Neurosci* **16**, 2701–2715.

Kawaguchi Y & Kubota Y (1997). GABAergic cell subtypes and their synaptic connections in rat frontal cortex. *Cereb Cortex* **7**, 476–486.

Kawaguchi Y & Kubota Y (1998). Neurochemical features and synaptic connections of large physiologically identified GABAergic cells in the rat frontal cortex. *Neuroscience* **85**, 677–701.

Klausberger T, Magill PJ, Marton LF, Roberts JD, Cobden PM, Buzsaki G & Somogyi P (2003). Brain-state- and cell-type-specific firing of hippocampal interneurons in vivo. *Nature* **421**, 844–848.

Klausberger T, Marton LF, Baude A, Roberts JD, Magill PJ & Somogyi P (2004). Spike timing of dendrite-targeting bistratified cells during hippocampal network oscillations in vivo. *Nat Neurosci* **7**, 41–47.

Klausberger T, Marton LF, O'Neill J, Huck JH, Dalezios Y, Fuentealba P, Suen WY, Papp E, Kaneko T, Watanabe M, Csicsvari J & Somogyi P (2005). Complementary roles of cholecystokinin- and parvalbumin-expressing GABAergic neurons in hippocampal network oscillations. *J Neurosci* **25**, 9782–9793.

Korngreen A, Kaiser KM & Zilberter Y (2005). Subthreshold inactivation of voltage-gated K^+ channels modulates action potentials in neocortical bitufted interneurones from rats. *J Physiol* **562**, 421–437.

Kubota Y & Kawaguchi Y (1997). Two distinct subgroups of cholecystokinin-immunoreactive cortical interneurons. *Brain Res* **752**, 175–183.

Lund JS (1973). Organization of neurons in the visual cortex, area 17, of the monkey (*Macaca mulatta*). *J Comp Neurol* **147**, 455–496.

Lund JS (1987). Local circuit neurons of macacque monkey striate cortex. I. Neurons of laminae 4C and 5A. *J Comp Neurol* **159**, 305–334.

Lund JS (1988). Anatomical organization of Macaque monkey striate visual cortex. *Ann Rev Neurosci* **11**, 253–288.

Lund JS & Lewis DA (1993). Local circuit neurons of developing and mature macaque prefrontal cortex: Golgi and immunocytochemical characteristics. *J Comp Neurol* **328**, 282–312.

Markram H & Tsodyks M (1996). Redistribution of synaptic efficacy between neocortical pyramidal neurons. *Nature* **382**, 807–810.

Markram H, Wang Y & Tsodyks M (1998). Differential signalling via the same axon of neocortical pyramidal neurons. *Proc Natl Acad Sci U S A* **95**, 5323–5328.

Martina M, Schultz JH, Ehmke H, Monyer H & Jonas P (1998). Functional and molecular differences between voltage-gated K^+ channels of fast-spiking interneurons and pyramidal neurons of rat hippocampus. *J Neurosci* **18**, 8111–8125.

Martinotti C (1889). Contributo allo studio della corteccia cerebrale, ed all'origine central dei nervi. *Ann Reniatr Sci Affini* **1**, 314–381.

Monyer H & Markram H (2004). Interneuron Diversity series: Molecular and genetic tools to study GABAergic interneuron diversity and function. *Trends Neurosci* **27**, 90–97.

Porter JT, Cauli B, Staiger JF, Lambolez B, Rossier J & Audinat E (1998). Properties of bipolar VIPergic interneurons and their excitation by pyramidal neurons in the rat neocortex. *Eur J Neurosci* **12**, 3617–3628.

Ramón y Cajal S (1911). *Histologie de systeme nerveux de l'Homme et des vertebres tomme II.* Maloine, Paris.

Reyes A, Lujan R, Rozov A, Burnashev N, Somogyi P & Sakmann B (1998). Target-cell-specific facilitation and depression in neocortical circuits. *Nat Neurosci* **1**, 279–285.

Rozov A, Jerecic J, Sakmann B & Burnashev N (2001). AMPA receptor channels with long-lasting desensitization in bipolar interneurons contribute to synaptic depression in a novel feedback circuit in layer 2/3 of rat neocortex. *J Neurosci* **21**, 8062–8071.

Somogyi P (1977). A specific 'axo-axonal' interneuron in the visual cortex of the rat. *Brain Res* **136**, 345–350.

Somogyi P & Klausberger T (2005). Defined types of cortical interneurone structure space and spike timing in the hippocampus. *J Physiol* **562**, 9–26.

Tamas G, Buhl EH & Somogyi P (1997). Fast IPSPs elicited via multiple synaptic release sites by different types of GABAergic neurone in the cat visual cortex. *J Physiol* **500**, 715–738.

Thomson AM (2003). Presynaptic frequency- and pattern-dependent filtering. *J Comput Neurosci* **15**, 159–202.

Thomson AM, Bannister AP, Hughes DI & Pawelzik H (2000). Differential sensitivity to Zolpidem of IPSPs activated by morphologically identified CA1 interneurones in slices of rat hippocampus. *Eur J Neurosci* **12**, 425–436.

Thomson AM, Deuchars J & West DC (1993). Single axon EPSPs in neocortical interneurones exhibit pronounced paired pulse facilitation. *Neuroscience* **54**, 347–360.

Thomson AM & West DC (2003). Presynaptic frequency filtering in the gamma frequency band; dual intracellular recordings in slices of adult rat and cat neocortex. *Cereb Cortex* **13**, 136–143.

Thomson AM, West DC & Deuchars J (1995). Properties of single axon EPSPs elicited in spiny interneurones by action potentials in pyramidal neurones in slices of rat neocortex. *Neuroscience* **69**, 727–738.

Thomson AM, West DC, Hahn J & Deuchars J (1996). Single axon IPSPs elicited in pyramidal cells by three classes of interneurones in slices of rat neocortex. *J Physiol* **496**, 81–102.

Toledo-Rodriguez M, Goodman P, Illic M, Wu C & Markram H (2005). Neuropeptide and calcium-binding protein gene expression profiles predict neuronal anatomical type in the juvenile rat. *J Physiol* **567**, 401–413.

Tsodyks MV & Markram H (1997). The neural code between neocortical pyramidal neurons depends on neurotransmitter release probability. *Proc Natl Acad Sci U S A* **94**, 719–723.

Wang Y, Gupta A, Toledo-Rodriguez M, Wu CZ & Markram H (2002). Anatomical, physiological, molecular and circuit properties of nest basket cells in the developing somatosensory cortex. *Cereb Cortex* **12**, 395–410.

Wang Y & Ramage AG (2001). The role of central 5-HT_{1A} receptors in the control of B-fibre cardiac and bronchoconstrictor vagal pregandglionic neurones in anaesthetized cats. *J Physiol* **536**, 753–767.

Wang Y, Toledo-Rodriguez M, Gupta A, Wu C, Silberberg G, Luo J & Markram H (2004). Anatomical, physiological and molecular properties of Martinotti cells in the somatosensory cortex of the juvenile rat. *J Physiol* **561**, 65–90.

West DC, Mercer A, Kirchhecker S, Morris OT & Thomson AM (2006). Layer 6 cortico-thalamic pyramidal cells preferentially innervate interneurons and generate facilitating EPSPs. *Cereb Cortex* **16**, 200–211.

Xiang Z, Huguenard JR & Prince DA (2002). Synaptic inhibition of pyramidal cells evoked by different interneuronal subtypes in layer 5 of rat visual cortex. *J Neurophysiol* **88**, 740–750.

Acknowledgements

This work was supported by the Medical Research Council (UK) and Novartis Pharma (Basel). Polyclonal antibodies were a kind gift from Professor K. Baimbridge, UBC, Canada.

Author's present address

A. P. Bannister: Department of Clinical Neuropathology, Academic Neurosciene Building, Kings College Hospital Denmark Hill, London SE5 9RS, UK.

Supplemental material

The online version of this paper can be accessed at:
DOI: 10.1113/jphysiol.2006.124214
http://jp.physoc.org/cgi/content/full/jphysiol.2006.124214/DC1
and contains supplemental material consisting of six figures.

Supplementary Figure 1. A large fast, continuous spiking parvalbumin-immunopositive interneurone in layer 4 of cat visual cortex elicits a fast IPSP in a layer 4 pyramidal cell.

Supplementary Figure 2. A strongly adapting/burst firing parvalbumin-immunonegative double bouquet interneurone in layer 4 of cat visual cortex elicits IPSPs in two postsynaptic layer 4 pyramidal cells.

Supplementary Figure 3. A narrow spike, stopping/stuttering multipolar interneurone in layer 4 of cat visual cortex elicits fast IPSPs in a postsynaptic layer 5 pyramidal cell.

Supplementary Figure 4. A large, narrow spike, stopping/stuttering multipolar interneurone in layer 4 of cat visual cortex elicits large, fast IPSPs in a postsynaptic layer 4 spiny stellate cell.

Supplementary Figure 5. A slow spiking, stopping/stuttering bipolar interneurone in layer 4 of cat visual cortex is reciprocally connected to a postsynaptic layer 4 pyramidal cell.

Supplementary Figure 6. Evidence for a presynaptic locus for synaptic facilitation and depression and correlations with EPSP time course.

This material can also be found as part of the full-text HTML version available from http://www.blackwell-synergy.com